AIP | Journal of Applied Physics

Modulation of the magnetic/conductive dead layer at the manganites-SrTiO3 interface

W. W. Gao, F. X. Hu, B. G. Shen, and J. R. Sun

Citation: Journal of Applied Physics **117**, 17C733 (2015); doi: 10.1063/1.4916297
View online: http://dx.doi.org/10.1063/1.4916297
View Table of Contents: http://scitation.aip.org/content/aip/journal/jap/117/17?ver=pdfcov
Published by the AIP Publishing

Modulation of the magnetic/conductive dead layer at the manganites-$SrTiO_3$ interface

W. W. Gao,[1,2] F. X. Hu,[1] B. G. Shen,[1] and J. R. Sun[1,a)]
[1]*Beijing National Laboratory for Condensed Matter Physics, Institute of Physics, Chinese Academy of Sciences, Beijing 100190, People's Republic of China*
[2]*Department of Electrical Engineering and Computer Sciences, University of California, Berkeley, California 94720, USA*

(Presented 5 November 2014; received 22 September 2014; accepted 27 October 2014; published online 26 March 2015)

We presented a systematic study on the transport properties of the $La_{0.67}A_{0.33}MnO_3$ (LAMO) (A = Ba, Ca) and $La_{0.67}Ca_{0.33}MnO_3/LaMnO_3$ (LCMO/LMO) films with the LAMO layer of the thickness from 0 to 50 nm and a fixed LMO thickness of 3 nm. An interface layer with degenerated magnetic and conductive properties has been observed. It is interesting that the dead layer in LBMO is much thinner than that in LCMO. The thickness for the dead layer is, deduced from the conductivity-film thickness relation at 5 K, ~6 nm for LCMO and ~3 nm for LBMO, essentially weakly dependent of magnetic field. After introducing the LMO buffer layer, the magnetic field dependence is considerably enhanced; a simple estimate indicates that a field of 5 T depresses the layer thickness from ~6 nm to ~3 nm. It indicates that the LMO layer enhances the sensitivity of trapped charge carriers at the interface to magnetic field, thus activates the dead layer. © *2015 AIP Publishing LLC*. [http://dx.doi.org/10.1063/1.4916297]

I. INTRODUCTION

The surface/interface properties of the manganite films are different from those of the bulk. They become particularly important when interfacial process, such as interface layer coupling and transport, which dominates the properties of multilayer structured materials.[1–3] Because of the order-disorder transition of the spin, charge, and orbital charge degrees of freedom, and strong magnetic-conductive coupling existing in the manganites,[4,5] the magnetic field is expected to have an important effect on the various behaviors of the manganites. However, the magnetic field effects have been severely depressed by the strong surface/interface effect. The magnetic degeneration of the surface layer in manganite films[6] and the presence of a magnetic/conductive dead layer at the manganite/substrate had been reported.[3] The occurrence of phase separation, due to lattice distortions and related structure defects, probably leads to the degeneration of interfacial properties.

In order to incorporate the excellent properties of the manganites into corresponding devices, the interfacial layer must be activated. Yamada *et al.*[7] found the interfacial ferromagnetism of the $La_{0.6}Sr_{0.4}MnO_3$ film on $SrTiO_3$ (STO) can be recovered by introducing $LaMnO_3$ buffer layer. As reported, the buffer layer enhanced positive magnetoresistance (MR) can be observed in manganite-based junctions.[8–11] Besides, the interface layer was found to be easily tuned by external stimuli such as magnetic field, electric voltage, lattice strain, and charge exchange existing between film and substrate.[3,12,13] Up to now, the reports on the interface dead layer are still limited due to its insulating behavior and depressed magnetization, which hinders both the electric transport and magnetic measurements. It is completely essential to study the modulation of magnetic-conductive dead layer of manganites films.

In this paper, we will present a systematic study on the magnetic transport properties in the $La_{0.67}A_{0.33}MnO_3$ (LAMO) (A = Ba, Ca) and $La_{0.67}Ca_{0.33}MnO_3/LaMnO_3$ (LCMO/LMO) films with the LAMO layer of the thickness from 0 to 50 nm and a fixed LMO thickness of 3 nm. An interface layer with degenerated magnetic and conductive properties has been observed. It is interesting that the dead layer in LBMO is much thinner than that in LCMO. However, they are weakly dependent of magnetic field. After introducing a LMO buffer layer, the magnetic field response of interface layer is considerably enhanced; a simple estimate indicates that a field of 5 T depresses the layer thickness from ~6 nm to ~3 nm. It indicates that the LMO layer enhances the sensitivity of trapped charge carriers at the interface to magnetic field, thus activates the dead layer.

II. EXPERIMENTAL PROCEDURE

Three series of manganese oxides films were fabricated by growing, via the pulsed laser ablation technique, LAMO (A = Ba, Ca) monolayer, and LCMO/LMO(3 nm) bilayers on (001)-oriented STO substrates. During the deposition process, temperature of the substrate was kept at 720 °C and the oxygen pressure at ~10 Pa, for the LMO film, ~60 Pa, for the LBMO film, and ~80 Pa, for LCMO film. The sample size is 3 × 5 mm^2, and the manganite film thickness is from 0 to 50 nm. The film thickness was controlled by the number of laser pulses. In order to determine the thickness of ultrathin films, the deposition rate was carefully calibrated: Three standard LMO, LBMO, and LCMO films were first prepared

a)Author to whom correspondence should be addressed. Electronic mail: jrsun@iphy.ac.cn.

under the above condition, then parts of the films were removed from the substrate by conventional lithographic technique and the sharp film edge thus formed were measured by atomic force microscope (AFM). In this way, an accurate correspondence between pulse number and film thickness was established. The crystal structure of films was analyzed by x-ray diffraction (XRD). The film surface morphology was investigated by AFM. The transport measurements were performed by Physical Property Measurement System (PPMS), using the standard four-point technique.

III. RESULTS AND DISCUSSIONS

The surface topography of the manganite films were investigated by AFM. The films are very smooth and the root-mean-square roughness of the films varies between ~0.2 and ~0.5 nm. Figs. 1(a)–1(c) present the typical AFM images of the LMO buffer layer of 3 nm, LBMO and LCMO films with the thicknesses of 30 nm, respectively. Terrace-structured surface structure with a step of ~0.4 nm is observed in the LMO buffer layer, signifying a layer by layer growth of the films. This will guarantee the high quality of the top LCMO films in Fig. 1(d). The top LCMO film is still quite smooth, no visible difference between LCMO and LCMO/LMO is observed.

The crystal structure of manganite films was presented by XRD technique. Figs. 2(a) and 2(b) show the XRD patterns recorded around the (002) peak (indexed based on the cubic perovskite structure) of the LBMO, LCMO, and LCMO/LMO(3 nm) with LAMO thickness of 35 nm. The XRD peak of the LBMO film is very close to that of STO substrate and unidentifiable when the film thickness is below 40 nm. Comparing with LCMO, the XRD peak of LCMO/LMO shifts to lower angle, indicating the increase in lattice parameter.

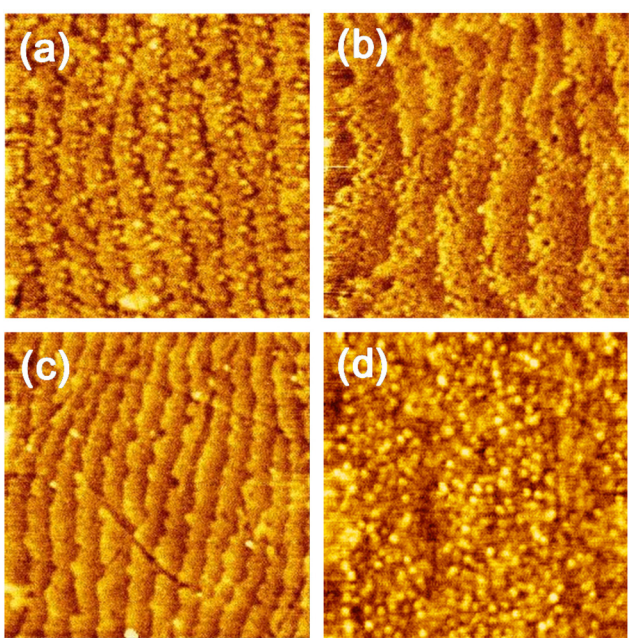

FIG. 1. (a) Surface topography of the LBMO, (b) LMO(3 nm) buffer layer, (c) LCMO, and (d) LCMO/LMO(3 nm) film with the LAMO thickness of 30 nm. The scale of the image is $1 \times 1\ \mu m^2$.

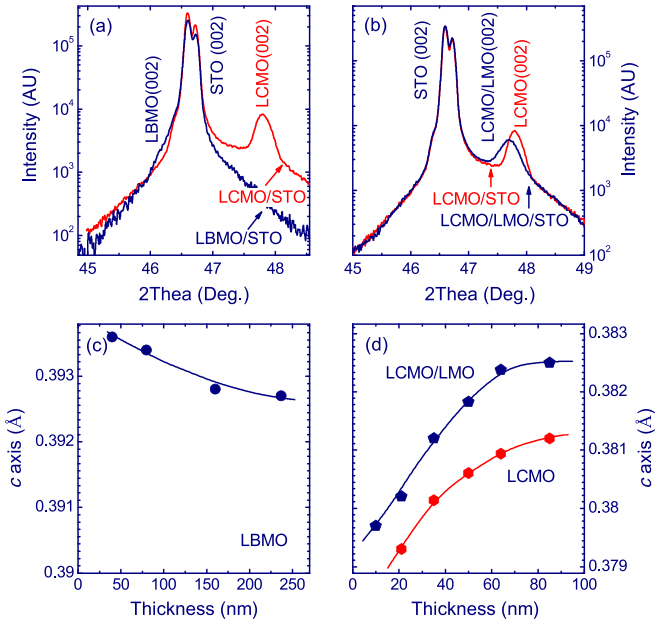

FIG. 2. (a) and (b) The XRD pattern of the LBMO, LCMO, and LCMO/LMO(3 nm) films with the LAMO thickness of 35 nm, recorded around the (002) peak. (c) and (d) Film thickness dependent of out-of-plane lattice parameter of LBMO, LCMO, and LCMO/LMO(3 nm) films. Solid lines are guides for the eyes.

The lattice parameters of three series films along the *c*-axis were calculated from (002) peak position, and thickness dependence relations are shown in Figs. 2(c) and 2(d). The *c* values are considerately larger and smaller than that of the bulk for LBMO and LCMO, respectively. With increasing LBMO film thickness, the *c*-axis value diminished slowly, the film is not relaxed completely, even in the thickness up to 240 nm. In contrast, the lattice parameter of LCMO rapidly increases to ~3.812 Å as film thickness grows from 10 to 80 nm and approaches the saturated value above 80 nm, indicating the relaxation of the tensile strains of the films. After introducing the LMO buffer layer, the lattice parameter increases and reaches to saturate more quickly.

Figs. 3(a) and 3(b) present a summary of the temperature-dependent on the resistivity of the LBMO and LCMO films, measured by the standard four-probe technique, alone the manganites films plane with an applied current of 1 μA. The resistance of the films was also measured under a constant current of 0.1 μA, and no visible difference is obtained. During cooling down process, the resistivity of both LBMO and LCMO films undergoes first an exponential growth, above a character temperature T_p, then a rapid decrease, which is a typical insulator-metal transition behavior of the manganite films. The LCMO films show a rapidly increase in resistivity upon thickness reduction due to the stronger Jahn-Teller distortion, also accompanying with the decrease in T_p. In contrast, LBMO film shows a slower increase in resistivity, and T_p can still be identified in the LBMO film of 4 nm. Here, the LBMO and LCMO exhibit different lattice mismatch with STO substrate, which is ~−0.15% for the LBMO films and ~1.2% for the LCMO films. Obviously, the different strain types have no visible impact on the increase in resistivity.

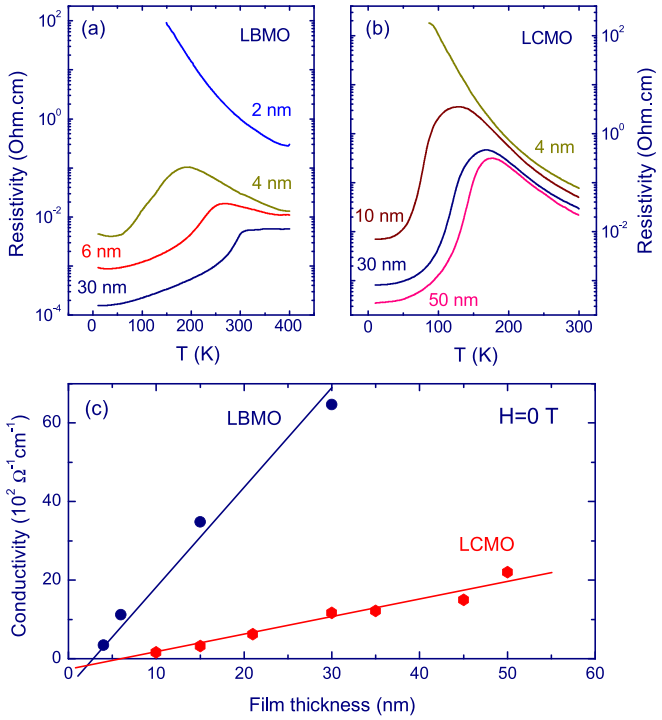

FIG. 3. Temperature dependence of the lateral resistivity of the LBMO (a) and LCMO (b) films on the STO substrate. (c) Conductivity as a function of film thickness at low temperature. Solid lines are guides for the eyes.

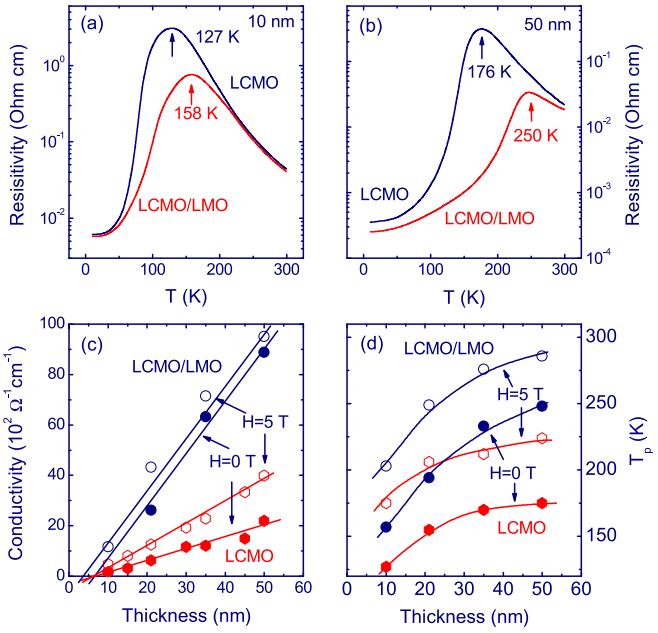

FIG. 4. Temperature dependence of the resistivity of the LCMO and LCMO/LMO(3 nm) on STO with LCMO thickness of 10 nm (a) and 50 nm (b), respectively. (c) Conductivity as a function of LCMO and LCMO/LMO(3 nm) film thickness. (d) T_p as a function of film thickness. Solid lines are guides for the eyes.

The increase in resistivity with decreasing film thickness indicates the presence of an interface dead layer with reduced conductivity. This can be seen clearly by thickness dependence of the film's conductivity (defined as conductivity = 1/resistivity), as shown in Fig. 3(c). The conductivity displays a linear reduction with decreasing thickness. The effective thickness of the dead layer can be obtained from the conductivity-thickness relation.[2] It is interesting that the dead layer in LBMO is much thinner than that in LCMO, about $\sim 3 \pm 0.6$ nm for LBMO film and $\sim 6 \pm 1.0$ nm for LCMO film, respectively, in the low temperature limit $T \rightarrow 0$. However, no conductive dead layer is observed at the room temperature (results not shown). The Jahn-Teller distortion due to larger lattice strain probably depresses the interface charge exchange and leads to a thicker dead layer. Besides, the electric transport is also studied in the presence of a field of 5 T and the thickness of dead layer shows weakly dependent of magnetic field (results not shown). It indicates that magnetic field effect is deeply depressed by inactive interface layer. It is truly essential to consider how to modify the interfacial state and further active interface layer.

In order to active the interface process, a proper buffer layer is introduced between manganite film and substrate. As reported, the positive MR can be found in manganite-based heterojunctions by introducing a LMO buffer layer. Also the magnetic response is strongly dependence on the LMO layer thickness, maximized when the layer thickness is ~3 nm. So the LMO layer with thickness of 3 nm is chosen in this paper.

Figs. 4(a) and 4(b) present the temperature dependence of the resistivity of the LCMO and LCMO/LMO with different LCMO thickness. The resistivity is measured by the standard four-probe technique under a constant current of 1 μA. An obvious decrease in resistivity and accompanied increase in T_p appear after adding LMO buffer layer. The change in T_p is ~31 K for 10 nm and ~74 K for 50 nm. As well established, the charge carries near the interface are localized by Jahn-Teller distortion due to lattice strain. The introduction of LMO buffer layer reduces the strain and awakens the depression of conductivity in manganite film.

The film thickness dependences on the conductivity are shown in Fig. 4(c). The interface dead layer thickness can be obtained by extrapolating the conductivity-thickness relation to conductivity→0. It is $\sim 6 \pm 0.8$ nm for LCMO/LMO film and almost same as the LCMO monolayer. Besides, the transport behavior is studied in the presence of a field of 5 T. It is interesting that its field dependence is considerably enhanced; a simple estimate indicates that a field of 5 T depresses the layer thickness from $\sim 6 \pm 0.8$ nm to $\sim 3 \pm 0.7$ nm. It indicates that the LMO layer enhances the sensitivity of trapped charge carriers at the interface to magnetic field, thus activates the dead layer. In contrast, the dead layer in LCMO monolayer displays weakly dependence on the magnetic field.

Fig. 4(d) presents T_p as a function of the LCMO and LCMO/LMO(3 nm) thickness. The peak around T_p can not be seen when the film thickness is close or below the dead layer. They display first a smooth then a fast decrease with the decrease in film thickness. Because of the incorporation of LMO layer, the T_p increases from ~127 K to ~158 K for 10 nm LCMO, and from ~176 K to ~250 K for 50 nm LCMO. With a field of 5 T, the T_p further increases to ~290 K, very close to room temperature. It indicates that the metal-insulator phase transition temperature can be tuned

from ~127 K to room temperature, even high temperature. It is meaningful and could be a potential application for manganite architecture.

IV. CONCLUSION

In conclusion, the magnetic transport properties of the LAMO (A = Ba, Ca) and LCMO/LMO films with different LAMO thickness have been studied systematically. An interface layer with degenerated magnetic and conductive properties has been observed. With the decrease in film thickness, an increase in resistivity and an accompanied decrease in resistive transition temperature appear, due to the presence of a conductive dead layer. The thickness for the dead layer is, deduced from the conductivity-film thickness relation at 5 K, $\sim 6 \pm 1.0$ nm for LCMO and $\sim 3 \pm 0.6$ nm for LBMO, essentially weakly dependent of magnetic field.

After introducing the LMO buffer layer, its magnetic field dependence is considerably enhanced, a simple estimate indicates that a field of 5 T depresses the layer thickness from $\sim 6 \pm 0.8$ nm to $\sim 3 \pm 0.7$ nm. It indicates that the LMO layer enhances the sensitivity of trapped charge carriers at the interface to magnetic field, thus activates the dead layer. Besides, the metal-insulator phase transition temperature can be tuned from ~127 K to room temperature, even high temperature, by the buffer layer and magnetic field.

ACKNOWLEDGMENTS

This work has been supported by the National Natural Science Foundation of China, the National Fundamental Research of China, and the Knowledge Innovation Project of the Chinese Academy of Sciences.

[1]W. D. Luo, S. J. Pennycook, and S. T. Pantelides, Phys. Rev. Lett. **101**, 247204 (2008).
[2]J. Z. Sun, D. W. Abraham, R. A. Rao, and C. B. Eom, Appl. Phys. Lett. **74**, 3017 (1999).
[3]J. R. Sun, B. G. Shen, Z. G. Sheng, and Y. P. Sun, Appl. Phys. Lett. **85**, 3375 (2004).
[4]P. Schiffer, A. P. Ramirez, W. Bao, and S.-W. Cheong, Phys. Rev. Lett. **75**, 3336 (1995).
[5]*Colossal Magnetoresistance Oxides*, edited by Y. Tokura (Gordon and Breach, London, 1999).
[6]J. H. Park, E. Vescovo, H. J. Kim, C. Kwon, R. Ramesh, and T. Venkatesan, Phys. Rev. Lett. **81**, 1953 (1998).
[7]H. Yamada, Y. Ogawa, Y. Ishii, H. Sato, M. Kawasaki, H. Akoh, and Y. Tokura, Science **305**, 646 (2004).
[8]W. W. Gao, J. R. Sun, X. Y. Lu, D. S. Shang, J. Wang, F. X. Hu, and B. G. Shen, J. Appl. Phys. **109**, 07C729 (2011).
[9]W. M. Lu, J. R. Sun, Y. Z. Chen, D. S. Shang, and B. G. Shen, Appl. Phys. Lett. **95**, 232514 (2009).
[10]W. W. Gao, W. M. Lü, A. D. Wei, J. Wang, J. Shen, B. G. Shen, and J. R. Sun, J. Appl. Phys. **111**, 07D711 (2012).
[11]W. W. Gao, L. Hu, Y. P. Sun, J. R. Sun, J. Shen, R. J. Chen, Y. F. Chen, and B. G. Shen, J. Appl. Phys. **113**, 17D716 (2013).
[12]Y. H. Sun, Y. G. Zhao, H. F. Tian, C. M. Xiong, B. T. Xie, M. H. Zhu, S. Park, W. Wu, J. Q. Li, and Q. Li, Phys, Rev. B **78**, 024412 (2008).
[13]S. Liang, J. R. Sun, J. Wang, and B. G. Shen, Appl. Phys. Lett. **95**, 182509 (2009).